2023 IEEE International Conference on Energy Technologies for Future Grids
Wollongong, Australia, December 3-6, 2023

Photovoltaics Maximum Power Tracking by the Hybrid Perturb-Observe and Sliding Mode Control Strategies

Nema Salem
Electrical and Computer Engineering Department
Effat University
Jeddah, Saudi Arabia
nsalem@effatuniversity.edu.sa
orcid.org/0000-0002-8440-4111

Eithar Alammari
Electrical and Computer Engineering Department
Effat University
Jeddah, Saudi Arabia
eioalammari@effat.edu.sa

Joud Alamro
Electrical and Computer Engineering Department
Effat University
Jeddah, Saudi Arabia
joalamro@effat.edu.sa

Sara Alashwali
Electrical and Computer Engineering Department
Effat University
Jeddah, Saudi Arabia
saalashwali@effat.edu.sa

***Abstract*—To increase photovoltaic PV power, the point of maximum power, MPPT, must be tracked effectively. The oscillation around the operating point is the main drawback of MPPT-obtaining techniques. This study suggests combining the Perturb and Observe, PO, and Sliding Mode Control, SMC, strategies to reduce this problem and deal with the nonlinearities of the solar panels under different climate situations. The SMC creates a sliding surface that establishes the operational point and increases the stability of the PO. The gate of a DC-DC converter quickly reaches this defined surface, and the duty cycle adjustment ensures maximum power in all conditions. This study utilized MATLAB/Simulink to design and analyze this combined control system. The outcomes supported the PO and SMC strategy's reliability and successful operation under various environmental circumstances.**

***Index Terms*—Sliding Mode Control, Perturb and Observe, Maximum Power-Point Tracking, Photovoltaics, PV**

I. INTRODUCTION

Alternative and green energy sources are viable replacements for fossil fuels like coal and natural gas. Green energy is produced from limitless resources without harming the environment or emitting gases, but alternative energy is produced from confined resources with the same advantages. Both have similar long-term objectives of lowering gas emissions and protecting the environment. Solar energy is the energy that photovoltaic cells in solar panels absorb from sunlight to build an electrical charge that travels in reaction to an internal electric field in the cell and generates electricity.

Since the sun continues to produce energy until it goes supernova, solar energy is a renewable energy source. Due to its widespread application in the commercial and residential sectors, photovoltaics are of considerable interest. Optimizing solar energy power generation became essential in order to improve the effectiveness of solar systems, reduce the number of panels needed to satisfy a particular load demand, and reduce total costs [1].

One of these optimization techniques is the Maximum Power-Point Tracking algorithm, MPPT. Over time, many MPPT algorithms have been developed to locate the MPPT and compel the system to operate at this point regardless of the environment [2]. Perturb and Observe (PO) and Sliding Mode Control (SMC) are two widely used techniques for MPPT in photovoltaic (PV) systems.

Due to its simplicity and cheap computing cost, the PO is one of the most used MPPT algorithms. The fundamental idea behind it is to alter the PV system's operational point and track any changes in output power that result. After then, based on the control modification, the direction of the perturbation is changed until the attainment of the MPP [3]. Although PO is simple and easy to implement, it has some drawbacks. One of the main disadvantages of it is that it can get trapped in local maxima and oscillate around the MPP. This phenomenon is the hunting effect and can decrease the system's efficiency.

SMC is another common MPPT technique that has lately received much attention. It is a nonlinear control method that is based on the idea of sliding modes. Designing a sliding surface that isolates the MPP from other operating points is the fundamental tenet of SMC. The system is subsequently driven toward the sliding surface and maintained there by the control law. SMC's ability to handle the non-linearity and uncertainty of the PV system is one of its primary benefits. SMC is also capable of handling quick and dynamic changes in system operating circumstances. SMC, however, needs more processing power and a more intricate control scheme than

PO. There are several advantages to using this controller with DC-DC converters, including its simplicity of use, robustness, and high dynamic response [4].

Several studies have compared the performance of PO and SMC in MPPT applications. In [5], The authors contrasted PO and SMC's effectiveness, tracking speed, and stability. Regarding efficiency and stability, the findings revealed that SMC beat PO but had a somewhat slower tracking speed. In [6],The authors introduced a photovoltaic MPPT that combined fuzzy logic control with current control modifiers like perturbation and observation. The algorithm's objective is to shorten the oscillation and the settling time. The findings showed that the time and power efficiency were 146 milliseconds and 99.5%, respectively. In [7], In order to anticipate the reference voltage under various weather situations, the scientists devised a deep-learning model that uses backpropagation to get maximum power points. In other scenarios, the results demonstrated that each panel was capable of producing ultimate power accuracy of 98% when compared to current techniques. In [8], The scientists suggested an adaptive neural-fuzzy inference approach to determine the solar systems' peak power. The ideal voltages are the output variables, whereas the irradiance and temperature are the input variables. In order to fine-tune the incremental conductance, they developed a hybrid whale optimization and pattern search approach. The outcomes demonstrate the appropriate operation of the suggested approach in various environmental settings with an efficiency of more than 99.3%. In [9], the authors suggested using a sliding mode controller to enhance the performance of a PV system's DC-DC boost converter. The MPPT algorithm-driven input voltage control loop and the current control loop, are designed to calculate the the inductor's current and the frequency's duty cycle of the switch, respectively. The findings demonstrated a decrease in steady-state error, overshoot, and settling time compared to lead-lag and PID controllers, proving its performance.

This study seeks to show the hybrid PO and SMC controllers' stability in tracking a PV system's MPPT under diverse climatic conditions. The following is how the paper is set up: Section II presents the properties of the solar panels, and Section III covers the modeling of a PV module. The design and analysis of the suggested system, including the development of the PO and SMC controllers and the DC-DC Boost converter, are shown in Section IV. In Section V, the simulation findings for the system under various irradiation conditions are discussed. In Section VI, findings are presented.

II. SOLAR PANELS CHARACTERISTICS

A photovoltaic array converts sunlight directly into energy through an electrical process in semiconductor materials. Solar energy can power electrical devices or provide electricity to the grid by forcing electrons from semiconductors to go via an electrical circuit. The solar system and its main components are shown in Fig. 1.

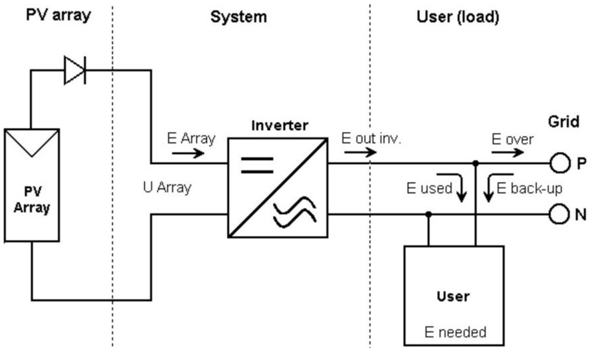

Fig. 1: The PV Solar System [10].

The ambient temperature and sun irradiation impact the solar panel's reaction. The solar cells' short-circuit current varies when the outside temperature increases. In contrast, the output power decreases due to a considerable drop in open-circuit voltage. Additionally, increasing the intensity of the sun's rays increases the output power and vice versa [11].

III. MODELING PV ARRAY

Fig. 2 depicts the circuit model of a solar array. The leakage current is expressed by a parallel resistance called R_{sh}, a light source called I_{ph}, a diode current called I_d, and a serial resistance called R_s." This model includes all instances where R_s denotes an internal resistance to the current flow. N_s is the number of photovoltaic cells connected in series, $V_t = Ak_bT/q$ is the diode thermal voltage, A is the diode quality factor, $k_b = \left(1.381 \times 10^{23} J/k\right)$ is Boltzmann's constant, $q = \left(1.602 \times 10^{-19} C\right)$ is the electron's charge, and T is the temperature under standard test conditions (in Kelvin). The calculation of the photovoltaic current is in (1).

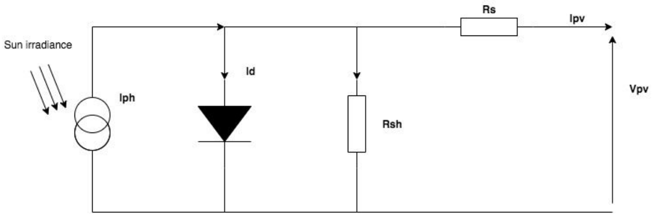

Fig. 2: The PV cell model.

$$I_{pv} = I_{ph} - I_d \left[exp\left(\frac{qV_{pv}}{k_bTA}\right) - 1\right] - \frac{V_{pv} + R_s I_{pv}}{R_{sh}} \quad (1)$$

IV. DESIGN AND ANALYSIS OF THE PROPOSED SYSTEM

Our proposed controlled solar system is depicted using MATLAB/Simulink in Fig. 3. We started by selecting the ASM6610P250W PV module with specifications shown in Table I [12], and Fig. 4 and 5.

A. Design of DC-DC Boost Converter

A DC-DC boost power converter, the second component of our system, is used as an adaptation step between the solar panel and the load to maximize solar power output. A power electronic converter called a DC-DC boost converter

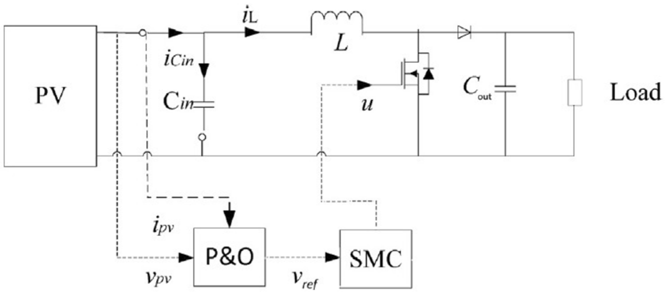

Fig. 3: The PV system using PO and SMC.

TABLE I: Specifications of the solar photovoltaic module.

Cell arrangement	6 × 10
V_{mp}	30.38 V
I_{mp}	8.29 A
I_{SC}	8.76 A
V_{OC}	37.12 V
Number of cells per module	60
V_{OC} temperature coefficient	-0.319
I_{SC} temperature coefficient	0.04
R_{sh}	508.8216 Ω
R_s	0.28598 Ω

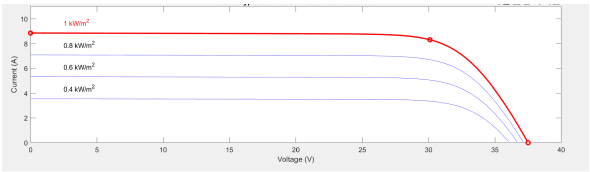

Fig. 4: IV characteristics of the ASM6610P250W PV module.

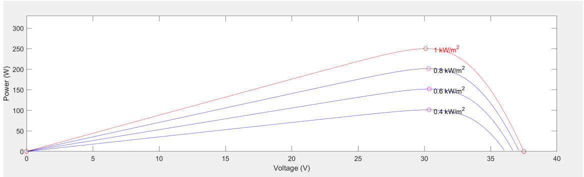

Fig. 5: PV characteristics of the ASM6610P250W PV module.

is frequently employed when a low-voltage source has to be raised in voltage. When a switch is on, the boost converter stores energy in an inductor. When the switch is off, the energy is released to the output. A DC-DC boost converter can be implemented using a variety of topologies. An inductor, a diode, a switch, and a capacitor make up the basic topology. Either a MOSFET or a BJT transistor can serve as the switch. Other topologies like the Cuk converter, the SEPIC converter, and the Zeta converter may also implement a boost converter [13].

Control is essential for a DC-DC boost converter to operate steadily and effectively. Many other control strategies have been proposed, including voltage mode control, peak current mode control, average current mode control, and pulse width modulation (PWM). In PWM control, the output voltage is regulated by varying the switch's on-time. The inductor current is measured and utilized to regulate the switch on time in current mode control. The output voltage is detected and utilized to control the switch on-time in voltage mode [14].

Considerations are made while designing a DC-DC boost converter, including component selection, control method preference, and converter efficiency optimization. The output power and required switching frequency determine the inductor and capacitor that should be used. The application's requirements, such as response time and stability, determine the control mechanism to be used. Minimizing component losses, such as those in the switch and the diode, is necessary to maximize converter efficiency.

The circuit's components in this research are the input and output capacitors C_{in} and C_{out}, the converter load R, and the inductor L [15]. The inductor current is denoted by i_L, the inductor voltage by V_L, the solar voltage by V_{pv}, the switch signal by u with a duty cycle of D, and $V_o = \frac{V_{pv}}{1-D}$ for the output voltage. The inductor value must be chosen for the optimal boost converter design following the constraint (2) such that the inductor current rating is larger than the photovoltaic current and assures the converter's stability. To stabilize the input voltage even with the switching power supply's peak current demand, the input capacitor value must be chosen following the constraint (3). The output capacitor value (4) is to have a voltage rating higher than the converter's output voltage, to carry the load current throughout the turn-on period, and the maximum ripple voltage to be 3%.

$$L \leq \frac{(1-D)^2 DR}{2 f_{sw}} \tag{2}$$

$$C_{in} \geq \frac{I_o D^2}{0.02(1-D) V_{in} f_{sw}} \tag{3}$$

$$C_{out} = \frac{D V_o}{V_r R f_{sw}} \tag{4}$$

f_{sw} is the switching frequency, I_o is the output current, V_{in} is the input voltage, and V_r is the capacitor's ripple voltage. In our study, we designed the converter with $L = 3E-3H, C_{in} = 100E-6F, C_{out} = 100E-6F, R = 60\Omega$, and $f_{sw} = 5000Hz$.

B. A Hybrid of PO and SMC MPPT Contrller

Fig. 3 demonstrates the PV system and the hybrid PO/SMC approach. The signal u is used by the controller to act directly on the boost converter transistor's switch [16]. Equation (5) displays the converter's performance.

$$\begin{aligned} &\text{ON-time:} \quad V_{pv} = V_L = L\frac{di_L}{dt} \\ &\text{OFF-time:} \quad V_{pv} = V_L = L\frac{di_L}{dt} + V_o \\ &\text{Converter's behavior:} \frac{di_L}{dt} = \frac{V_{pv} - V_o(1-u)}{L} \end{aligned} \tag{5}$$

The following is the fundamental procedure for tracking the MPP utilizing the hybrid PO and SMC approach. The PV system's operational point is disturbed by modifying a

DC-DC converter's duty cycle using the PO approach. It is noticeable that the PV system's output power has changed. If the power shift is positive, the operating point is changed using the PO technique in the same direction. The operating point is accommodated in the opposite direction using the SMC approach if the change in power is negative. By creating a sliding surface that isolates the MPP from other operating points, the SMC technique keeps the operating point at the MPP. The goal of the control law is to maintain the system's motion toward the sliding surface. The change in power is adjusted until it reaches zero when the operating point is at the MPP.

The hybrid PO and SMC method's design and execution include some factors, including the choice of the sliding surface, fine-tuning of the control parameters, and optimization of the converter efficiency. The choice of method and the specific design considerations depend on the application's requirements, such as the response time, accuracy, and complexity. Equation (6) proposes the SMC sliding surface. The sequence of the MPPT algorithm can be summarized as follows.

- Calculate $\frac{dS}{dt}$,
- If its value is negative, then make $u = 0$ and increase $\frac{dS}{dt}$ till being a zero value,
- If its value is positive, then make $u = 1$ and decrease $\frac{dS}{dt}$ till being a zero value,
- Repeat the algorithm.

$$S = (V_{pv} - V_{ref})\, G_1 + i_{Cin} G_2 \tag{6}$$

The gain constants G_1 and G_2 are present. S and $\frac{dS}{dt}$ must be zero for the suggested strategy to work. moving forward;

$$\frac{dS}{dt} = \left(\frac{dV_{pv}}{dt} - \frac{dV_{ref}}{dt}\right) G_1 + \frac{di_{Cin}}{dt} G_2 \tag{7}$$

$$i_{Cin} = i_{pv} - i_L = C_{in}\frac{dV_{Cin}}{dt} \Rightarrow \frac{dV_{Cin}}{dt} = \frac{i_{pv} - i_L}{C_{in}} \tag{8}$$

Substituting (8) into (7), we get:

$$\frac{dS}{dt} = \left(\frac{i_{pv} - i_L}{C_{in}} - \frac{dV_{ref}}{dt}\right) G_1 + \left(\frac{di_{pv}}{dt} - \frac{di_L}{dt}\right) G_2 \tag{9}$$

Substituting (5) into (9), we get:

$$\begin{aligned}\frac{dS}{dt} = &\left(\frac{i_{pv} - i_L}{C_{in}} - \frac{dV_{ref}}{dt}\right) G_1 \\ &+ \left(\frac{di_{pv}}{dt} - \frac{V_{pv}}{L} + \frac{V_o(1-u)}{L}\right) G_2 = 0\end{aligned} \tag{10}$$

Therefore, (10) describes the dynamic model of the SMC whose fulfillment of the suggested method is guaranteed by the appropriate selection of gain constants and DC-DC boost converter parameters.

V. RESULTS

Using the MATLAB/Simulink, under irradiation of G = [1000–600–400] W/m^2 with a decrease of 0.2 seconds each, and at a temperature of T = $25C^{\circ}$, we constructed the suggested system as shown in Fig. 6.

Fig. 7, 8, and 9 show the output voltage, current, and power, respectively. From this, we found the performance parameters are as follows. The settling time in the current, voltage, and power are 11.312 ms, 10.9 ms, and 13.703 ms, respectively. In addition, the maximum values of current, voltage, and power are 1.975A. 118V, and 239.1W, respectively. The system performance has no overshooting and achieved an efficiency of $\frac{239.1 \times 100}{250} = 95.64\%$.

VI. CONCLUSION

To calculate the MPPT of a PV system under various climatic situations, this study was created and simulated to demonstrate the toughness and stability of the hybrid PO and SMC controllers. The two benefits of this hybrid approach are the simplicity and cheap computing cost of the PO and the SMC's capability to handle nonlinearities and uncertainties. As evidenced by the results, the system enables quick and high-performance tracking of the MPPT. In steady conditions, there is no oscillation around the MPPT. Many power electronic systems depend on the DC-DC boost converter, whose design and regulation are crucial for achieving steady and effective operation. Last but not least, other PV systems may use the same analysis and design based on other DC-DC converter types.

REFERENCES

[1] Nobuyoshi Mutoh, Masahiro Ohno, and Takayoshi Inoue. "A method for MPPT control while searching for parameters corresponding to weather conditions for PV generation systems". In: *IEEE Transactions on industrial electronics* 53.4 (2006), pp. 1055–1065.

[2] Shiqiong Zhou et al. "A novel maximum power point tracking algorithms for stand-alone photovoltaic system". In: *International journal of control, automation and systems* 8 (2010), pp. 1364–1371.

[3] Manoharan Premkumar, Kanagarathinam Karthick, and Rayichandran Sowmya. "A review on solar PV based grid connected microinverter control schemes and topologies". In: *International Journal of Renewable Energy Development* 7.2 (2018), p. 171.

[4] Martin Steinberger, Martin Horn, and Leonid Fridman. *Variable-Structure Systems and Sliding-Mode Control*. Springer, 2020.

[5] T Logeswaran and A SenthilKumar. "A review of maximum power point tracking algorithms for photovoltaic systems under uniform and non-uniform irradiances". In: *Energy Procedia* 54 (2014), pp. 228–235.

[6] Anuchit Aurairat and Boonyang Plangklang. "An alternative perturbation and observation modifier maximum power point tracking of PV systems". In: *Symmetry* 14.1 (2022), p. 44.

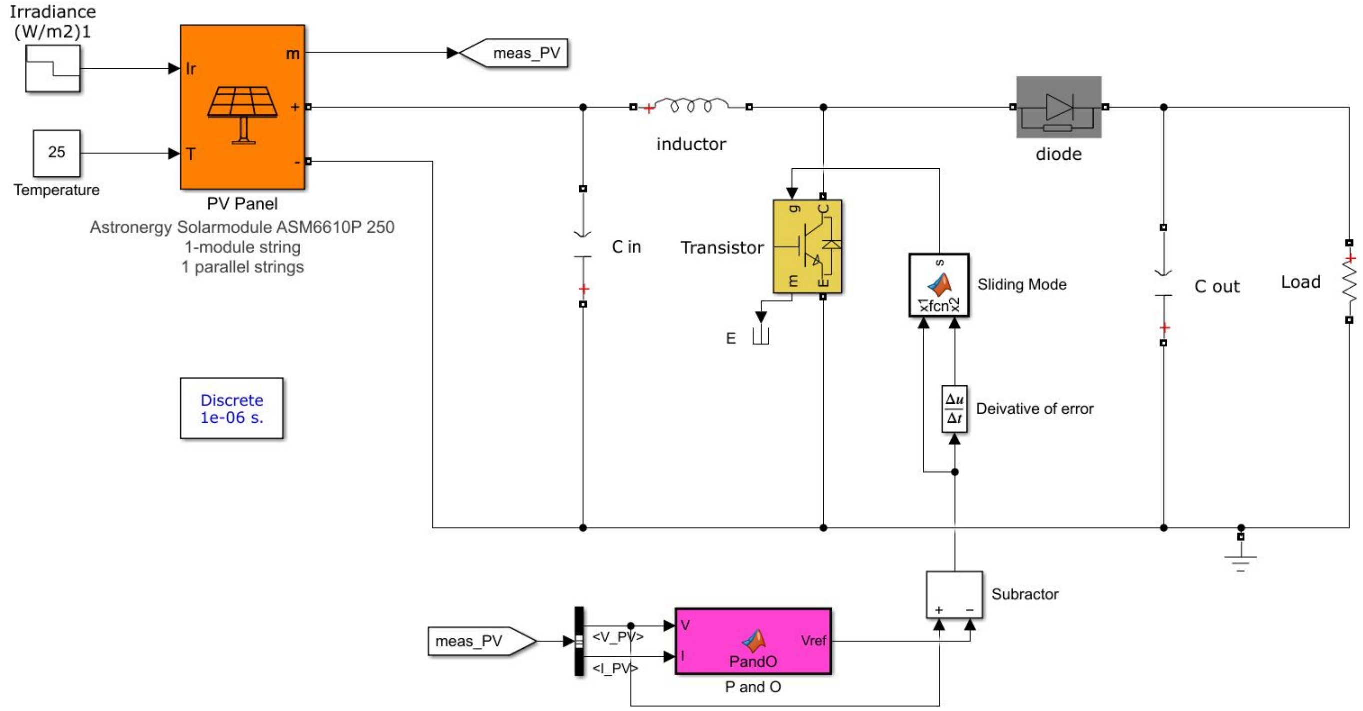

Fig. 6: Proposed system with MATLAB/Simulink.

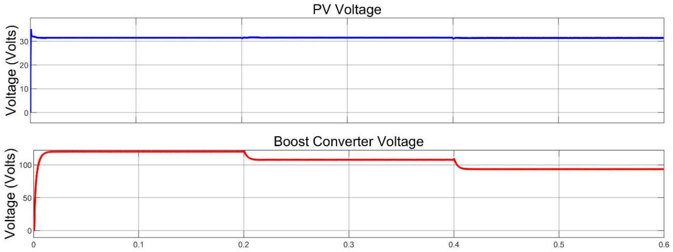

Fig. 7: The PV and converter output voltage.

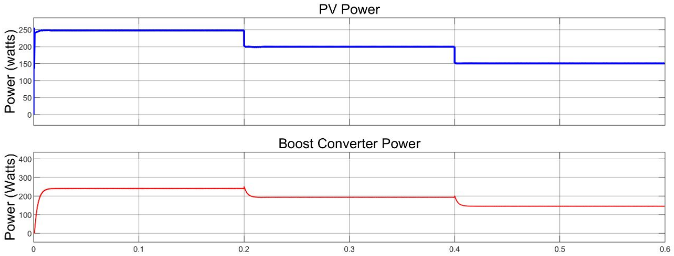

Fig. 9: The PV and converter output power.

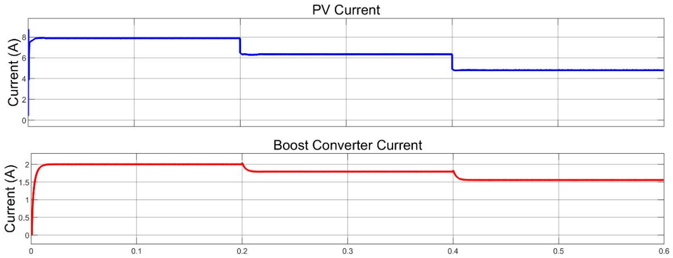

Fig. 8: The PV and converter output current.

[7] K Rafeeq Ahmed et al. “Maximum power point tracking of PV grids using deep learning”. In: *International Journal of Photoenergy* 2022 (2022).

[8] Mingxin Jiang et al. “A novel combinatorial hybrid SFL–PS algorithm based neural network with perturb and observe for the MPPT controller of a hybrid PV-storage system”. In: *Control Engineering Practice* 114 (2021), p. 104880.

[9] Roberto Sussumu Inomoto, José Roberto Boffino de Almeida Monteiro, and Alfeu J Sguarezi Filho. “Boost converter control of PV system using sliding mode control with integrative sliding surface”. In: *IEEE Journal of Emerging and Selected Topics in Power Electronics* 10.5 (2022), pp. 5522–5530.

[10] Nema Salem. “Design and Performance Analysis of a Grid-Connected Solar Power System for Energy Efficient AR Building”. In: (2023).

[11] Yaman Abou Jieb, Eklas Hossain, and E Hossain. *Photovoltaic systems: fundamentals and applications*. Springer, 2022.

[12] Astronergy. *Datasheet Crystalline PV Module ASM6610P(BF) Series*. Ed. by A Chnt company. URL: https://www.enfsolar.com/Product/pdf/Crystalline/5694705bdce76.pdf.

[13] Muhammad H Rashid. *Power electronics handbook*. Butterworth-heinemann, 2017.

[14] Shweta Dahale et al. “An overview of DC-DC converter topologies and controls in DC microgrid”. In: *2017 7th International Conference on Power Systems (ICPS)*. IEEE. 2017, pp. 410–415.

[15] Ameni Kchaou et al. “Second order sliding mode-based MPPT control for photovoltaic applications”. In: *Solar Energy* 155 (2017), pp. 758–769.

[16] Mostafa R Mostafa, Naggar H Saad, and Ahmed A El-sattar. “Tracking the maximum power point of PV array by sliding mode control method”. In: *Ain Shams Engineering Journal* 11.1 (2020), pp. 119–131.